21. PETROGRAPHY AND RELICT MINERALOGY OF SERPENTINITES FROM DEEP SEA DRILLING PROJECT LEG 84[1]

Sherman H. Bloomer, Scripps Institution of Oceanography[2]

ABSTRACT

Eleven serpentine samples from DSDP Leg 84 and four serpentinized ultramafic samples from Costa Rica and Guatemala were described and their relict mineral compositions measured by electron microprobe to try to determine the origin of the Leg 84 serpentinites and their relationship to the ultramafic rocks of the onshore ophiolites. The Leg 84 samples comprise more than 90% secondary minerals, principally serpentine, with hematitic and opaque oxides, and minor talc and smectites. Four distinct textural types can be identified according to the distribution of opaque phases and smectite. Remnants of spinel, olivine, orthopyroxene, and clinopyroxene occur variously in the samples; spinal occurs in all the samples. Textural evidence suggests that the serpentinites were originally clinopyroxene-bearing harzburgites. Relict mineral compositions are refractory and relatively uniform: olivine, $Fo_{90.6-90.9}$; orthopyroxene, En_{90-91}; clinopyroxene, Wo_{47} En_{50} Fs_3; spinels, Cr/Cr + Al = 0.4–0.6. 567A-29-2, 30–35 cm has slightly more magnesian olivines (Fo_{92}) and orthopyroxene, and more aluminous spinels (Cr/Cr + Al = 0.3). These compositions are similar to those inferred for refractory upper-mantle materials and also fall within the range of compositions for relict minerals in abyssal peridotites. They could be of oceanic origin. The onshore samples include serpentinites, a clinopyroxene-bearing harzburgite, and a clinopyroxenite. They too have magnesium-rich silicate assemblages, but relative to the drilled samples have more iron-rich olivines (Fo_{90}) and more aluminous and sodic pyroxenes; spinels which are clearly relicts are very aluminum-rich (Cr/Cr + Al = 0.1–0.25). These samples are most likely mantle materials, but significantly less depleted. Their relationship to the drilled samples is unclear. Serpentinites were the most common basement materials recovered during Leg 84, and there appears to be a bimodal assemblage (basalt/diabase and serpentine) of igneous rocks sampled from the trench slope. Diapirism of serpentine throughout the trench slope and forearc is suggested as an explanation for this distribution of samples.

INTRODUCTION

One of the objectives of DSDP Leg 84 was to sample the basement beneath the landward trench slope of the Middle America Trench off Guatemala. It had been suggested, on the basis of geophysical data, that this slope was composed of imbricated, landward-dipping slices of ocean crust (Seely et al., 1974; Ladd et al., 1978). Gravity and magnetic data, particularly a magnetic high parallel to the trench-slope break, are consistent with the presence of high-density crustal rocks at shallow depths, and indicate that these rocks may be an extension of mid-Tithonian–upper Santonian ophiolitic rocks exposed in coastal Costa Rica (Woodcock, 1975; Couch 1976; Couch and Woodcock, 1981). The recovery of clasts of serpentinite, basalt, and chert in cores and dredges along the trench slope supports this interpretation (Ibrahim et al., 1979).

On DSDP Leg 67, a partial transect was drilled across the trench and forearc, but the primary objective of drilling to basement in the nearshore slope was abandoned when large amounts of gas hydrated were encountered in the slope (von Huene, et al., 1980). The offshore slope is floored by basalts petrographically and chemically similar to normal ocean-ridge and spilitic ocean-ridge basalts (Maury et al., 1982); these are overlain by lower Miocene chalks (Coulbourn et al., 1982). The one onshore hole which penetrated basement (494A on the lower trench slope) yielded greenschist-facies metavolcanics which are similar to arc andesites or basaltic andesites in both clinopyroxene and bulk-rock chemistry (low Ti, Ni, high SiO_2 contents; Maury et al., 1982). These are overlain by Campanian–Maestrichtian limestones, indicating that this portion of trench is not currently undergoing accretion (Coulbourn et al., 1982).

The occurrence of Cretaceous sediments overlying basement in Hole 494A is another indication that there may be a relationship between the forearc basement and the upper Cretaceous ophiolitic rocks exposed on the Santa Elena, Nicoya, Oso, and Azuro peninsulas of Central America. The Nicoya Complex is a deformed volcaniclastic unit that includes metamorphosed pillow basalts overlain by chert and siliceous sediments; it was probably formed in mid-Tithonian to late Santonian time and emplaced in the margin in Santonian–Campanian time (Galli-Olivier, 1979). It was probably emplaced as a nappe, and was later uplifted in the Eocene–Oligocene (Kuijpers, 1980). The Nicoya Complex has been interpretated as oceanic material, on the basis of a very few analyses of basalts and the occurrence of pelagic sediments overlying the pillow basalts (Weyl, 1969; Pichler and Weyl, 1975). The Santa Elena Peninsula includes a complex of ultramafic rocks with some gabbros, thrust over a section of basic volcanic rocks; these two sections are separated by a breccia (Galli-Olivier, 1979; Azéma and Tournon, 1982). The peridotites are serpentinized harzburgites with olivine, orthopyroxene, brown spinel, and small amounts of clinopyroxene, and are cut by dikes of gabbro and dolerite (Azéma and Tournon, 1982).

[1] von Huene, R., Aubouin, J., et al., *Init. Repts. DSDP*, 84: Washington (U.S. Govt. Printing Office).

[2] Present address: Department of Geology, Duke University, Box 6729 College Station, Durham, NC 27708.

The volcaniclastic unit over which these are thrust may be an extension of the Nicoya Complex; it is overlain by Upper Cretaceous–Paleocene sediments with ultrabasic clasts (Azéma and Tournon, 1982).

Leg 84 was planned in part to complete the objective of Leg 67: to sample the basement of the trench slope and to examine the relationship between that basement and the onshore complexes. Indeed, at five of six sites, "ophiolitic"-type materials—most commonly serpentinites, with lesser amphibolitized gabbros and sheared metavolcanics—were recovered (site chapters, this volume). The oldest sediments recovered overlying this basement were upper Cretaceous limestone in Hole 567A, consistent with the age of ophiolitic rocks in Costa Rica.

The only primary minerals remaining in the serpentinite samples are scattered grains of olivine, orthopyroxene, clinopyroxene, and spinel. The compositions of those minerals provide the only information available to establish the initial compositional character of these serpentinites and the relationship of the Leg 84 serpentinites to the peridotites of the costal ophiolites. To that end, analyses of primary minerals in 11 samples from Leg 84 and 4 samples from the onshore ultramafic complexes of Central America are presented here.

SAMPLES AND METHODS

Cores from four of the five holes from which serpentinites were recovered (566, 567A, 566C, and 570) were examined, and samples which appeared to have some relict minerals were selected. The samples examined are listed in Table 1. Four samples from ultramafic outcrops in Guatemala and Costa Rica were also analyzed. CR-39 and CR-205 are a serpentinite breccia and a peridotite clast in a breccia, respectively, and are both from exposures along the Rio Potrero Grande in the Santa Elena Peninsula (samples supplied by N. Lundburg, University of California, Santa Cruz). D-50 and DL-90 are two Guatemalan peridotites similar in age to those in Costa Rica (approximately Barremian–Cenomanian, emplaced after the early Campanian; T. W., Donnelly, pers. comm., 1983). D-50 is from Minas de Oxec, Alta Verapaz (Rosenfeld, 1981); DL-90 is from Quebrada Patache, northeastern Sanarte Quadrangle (Lawrence, 1975); both were supplied by T. W., Donnelly, State University of New York Binghamton.

Table 1. Drilled samples used in this study, with textural type.

Sample (interval in cm)	Textural type[a]
566-6-1, 31–33	2, 3
566-9-1, 9–11	3
566C-6-1, 31–33	1
566C-7-1, 13–14	1
566C-7-1, 78–80	1
567A-28-1, 121–122	2, 3
567A-29-2, 30–35	3
567A-29-2, 140–142	2
570-42-1, 40–41	4
570-42-2, 53–55	4

[a] 1 = clear serpentine with reddish or orange spots.
2 = serpentine with abundant, fine-grained opaques, disseminated and in stringers.
3 = serpentine with dark gray to opaque sports or stains.
4 = clear serpentine with scattered, fine opaque grains and smectites.

Polished, 16-mm-diameter sections were prepared for each sample. Microprobe analyses were done on a Cameca CAMEBAX automated electron-probe microanalyzer with working conditions of 15 kV and 15 nA. Count time was 20s; spot size averaged 15 μm, but varied between 2 and 20 μm for some samples. Smithsonian and BRGM standards were used in the calibration. Modal analyses in Table 2 are approximate because of the very small area counted.

PETROGRAPHY

All the drilled samples can be termed serpentinites *sensu stricto*; all comprise greater than 90% secondary mineral assemblages dominated by serpentine (Table 2). The only clue to the original composition of the samples is in the few grains of unaltered primary minerals. Spinels are the most common of these relict grains, occurring in small percentages in all samples. They are red-brown to dark red-brown in thin section, range in size from 0.3 to 1.5 mm, and occur most commonly in elongate holly-leaf or anhedral habits and are fractured and broken (Fig. 1). In some samples there is a weak lineation, marked by elongation of single spinel grains and by alignments of groups of grains. Olivines are relatively uncommon as relict grains, reflecting their susceptibility to serpentinization. They occur as 0.1-mm clear, anhedral fragments, rarely with well-developed kink-bands suggesting an earlier, high-temperature deformation. Areas of simultaneous extinction among groups of relict grains define small (0.5-mm), decidely elongate areas in some samples. Orthopyroxene occurs as 0.4 to 1.4-mm relicts in bastites; although some have exsolution lamellae of clinopyroxene, well-developed lamellae are the exception rather than the rule. Most orthopyroxenes are completely replaced by bastite-type structures of clear serpentine, serpentine with semiparallel concentrations of opaques, or serpentine with linear exsolutions of dark reddish spinels. The correspondence of these bastite structures to replaced pyroxene is confirmed by the composition of the serpentine, which has distinctly higher contents of Cr and Al, and lower Ni, than does the adjacent massive serpentine. Such compositions indicate a pyroxene progenitor (Table 3). Many of the bastites are bent or broken (as indicated by opaque lamellae); some appear to have been

Table 2. Representative modal analyses of Leg 84 serpentinites and onshore peridotites (in vol.%).

	566C-7-1, 13–14 cm	566C-6-1, 31–33 cm	567A-29-2, 140–142 cm	570-42-1, 111–113 cm	DL90
Serpentine	88.6	75.2	90.7	75.8	12.1
Opaques	1.4	0.2	b	b	—[e]
Bastite	6.9	18.3	8.8	12.8	—
Olivine	—	1.2	—	0.8	72.5
Orthopyroxene	—	1.0	—	1.8	12.6
Spinel	0.1	1.0	0.3	0.7	0.8
Clinopyroxene	1.1	2.9	—	1.5	1.9
Veins	1.9	0.1	—	0.5	—
Other	—	0.2[a]	0.2[c]	6.2[d]	0.2[d]
Sum	100.0	100.1	10.0	100.1	100.1
% Secondary minerals	98.8	94.0	99.7	95.3	12.3

[a] Talc–tremolite.
[b] Abundant opaques, included with serpentine.
[c] Exsolution in bastite.
[d] Smectites.
[e] — indicates not detected.

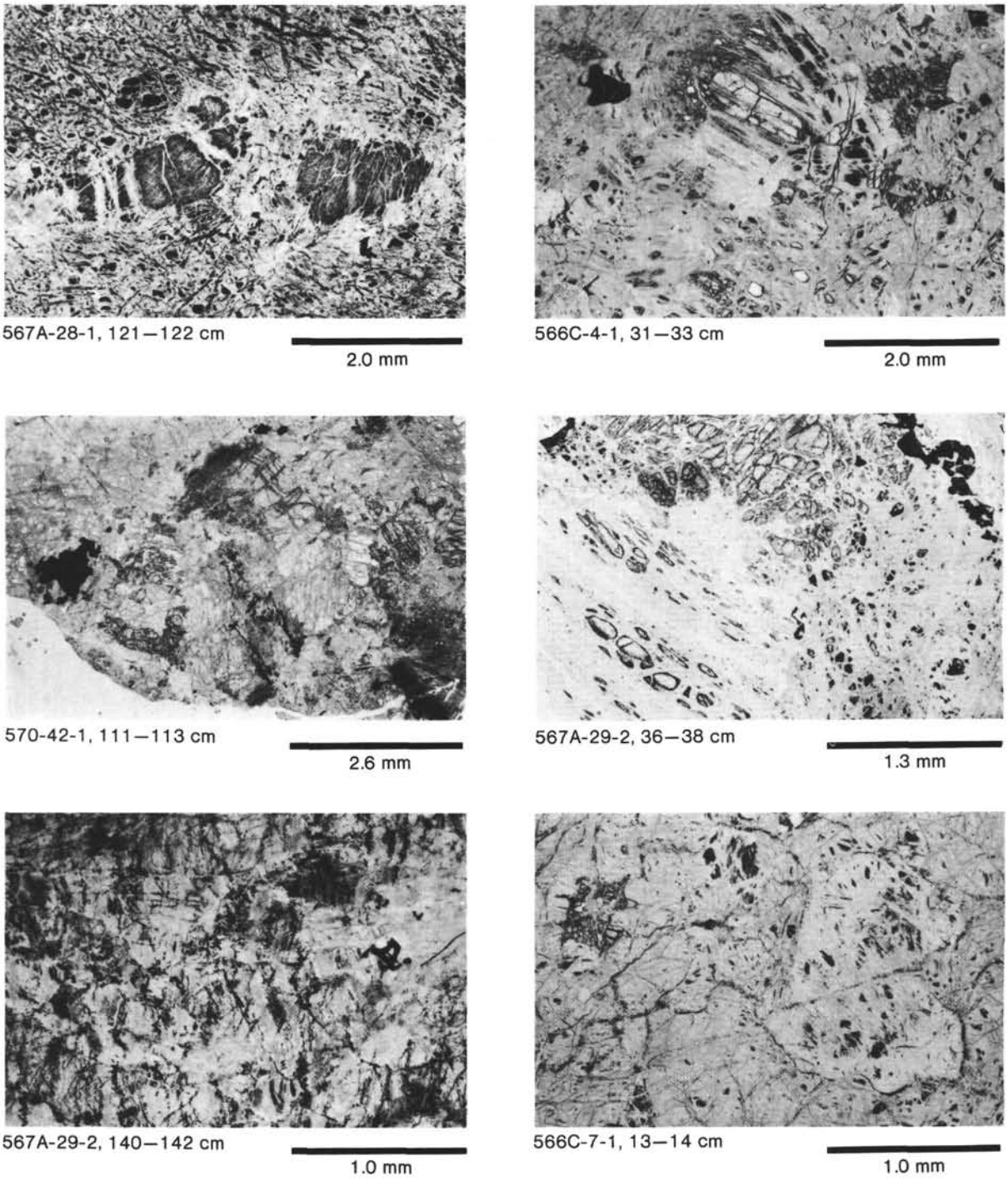

Figure 1. Photomicrographs of textures in serpentinites from Leg 84. Upper left, basite with spotty and disseminated opaques; upper right, clear serpentine with relict olivine, spinel, orthopyroxene, and clinopyroxene; middle left, Hole 570 sample with relict orthopyroxene and clinopyroxene and patches of greenish brown smectites; middle right, serpentine with some opaque spots, relict olivine, spinel, and orthopyroxene; lower left, serpentinite with abundant, disseminated opaques, one relict spinel; lower right, serpentinite with opaque spots, bastite, and relict clinopyroxene.

sheared into slightly elongate patches (Fig. 1). There are minor amounts of hydrogarnet developed in some samples. Clinopyroxene, when it occurs, appears to be quite resistant to serpentinization, and occurs as 0.1 to 0.8-mm anhedral, fractured grains. Well-developed exsolution lamellae of orthopyroxene are not common. The clinopyroxenes most often are associated with bastite pseudomorphs, which may occur in clumps of 2 to 5. The clinopyroxene appears to be a part of the original, equilibrium mineral assemblage in the rock.

The serpentine is pale green, typically with a meshwork structure, though fibrous serpentine is not uncommon. Veins of clear serpentine often cut through the meshwork matrix. Talc occurs in some of the bastites,

Table 3. Analyses of secondary materials in Leg 84 serpentinites.

	570-42-2, 53–55 cm			567A-29-2, 30–35 cm		
	Serpentine/ smectite	Serpentine		Talc/ serpentine	Serpentine	
		Bastite	Massive		Bastite	Massive
SiO_2	36.22	36.04	37.55	44.17	34.68	38.33
TiO_2	0.00	0.01	0.03	0.03	0.04	0.00
Al_2O_3	0.46	0.86	0.07	3.43	2.41	0.55
FeO^T	11.9	5.87	4.29	4.00	5.21	4.68
MnO	0.09	0.09	0.13	0.06	0.16	0.15
MgO	34.43	37.10	38.46	34.07	36.88	38.02
CaO	0.10	0.23	0.14	0.08	0.19	0.14
Na_2O	0.1	0.08	0.09	0.15	0.01	0.02
K_2O	0.06	0.03	0.03	0.03	0.02	0.05
P_2O_5	0.00	0.04	0.00	0.01	0.00	0.04
NiO	0.14	0.11	0.46	0.12	0.03	0.33
Cr_2O_3	0.15	0.64	0.03	0.58	0.61	0.01
Total	83.65	81.11	81.29	86.73	80.25	82.32

Note: T = total iron as FeO.

particularly those which include some relict orthopyroxene, but tremolite was not identified in any of these samples.

There are four distinct textural varities of serpentinite, distinguished principally on the basis of secondary opaque phases. The first type comprises a very clear, pale green serpentine with scattered grains of a blood-red, translucent mineral, most probably hematitic in composition (Fig. 1). Similar hematitic material occurs in veins in all textural types. The second variety has pale serpentine with discrete (0.03–0.2 mm) dark to opaque patches, probably a result of varying concentrations of opaque phases (Fig. 1). The third type has abundant (up to 15 modal %) fine-grained (<0.03 mm), disseminated opaque phases. There are samples which grade in texture between the latter two types. These differences in texture may reflect local differences in oxygen fugacities and water/rock ratios during serpentinization. The textural type to which each sample corresponds is keyed in Table 1. Samples from Site 570 exhibit a fourth texture, in which low-temperature retrograde metamorphism has produced crosscutting patches and veins of green to pale brown smectite, in a clear serpentine with a few scattered opaques.

Though these samples are serpentinized, the distribution of bastite pseudomorphs and relict orthopyroxene and clinopyroxene indicates that most were probably clinopyroxene-bearing harzburgites before serpentinization. Spinel probably made up 0.1–1 modal %, orthopyroxene 10–20%, clinopyroxene 1–3%, and olivine 76–89% of the original rocks. Despite more extensive serpentinization, the drilled samples are similar in texture to materials from Santa Elena described as "serpentinized harzburgitic peridotite showing relicts of olivine, orthopyroxene, brown spinel and, less frequently, clinopyroxene" (Azéma and Tournon, 1982).

The onshore samples are petrographically more diverse than the drilled samples. CR-39 is a clast-supported breccia with lithic serpentine fragments ranging in size from pebbles to fine sand. Opaque spinels are the only relict minerals identifiable, and the interpretation of some of these as relict is suspect. CR-205 is a clast from a similar breccia, and is a pale green-brown serpentinite with scattered opaques. There are abundant 0.1 to 1-mm olivine remnants that commonly occur as single grains or in groups of grains defining 0.7-mm-wide extinction areas; kink-bands are also common. Orthopyroxene occurs as large grains (up to 5 mm) with exsolution lamellae and spinel and clinopyroxene inclusions. It more commonly occurs as 0.5- to 1-mm grains which are distinctly undulose. Clinopyroxene occurs as smaller, anhedral grains with some exsolution lamellae of orthopyroxene; spinels are small and greenish brown with black rims.

DL-90 is a less serpentinized clinopyroxene-bearing harzburgite whose modal analysis is quite similar to the estimates for the original mineralogy of the drilled samples (Table 2). It comprises large (0.1–6 mm) interlocking olivine grains and lesser orthopyoxene grains cut by a meshwork of serpentine. The olivines are undulose, commonly have well-developed kink-bands, and show much grain-boundary recrystallization. The orthopyroxenes have few exsolution lamellae, and are often kinked and bent. Anhedral 1- to 3-mm clinopyroxenes with fine exsolution lamellae occur interstitially between the olivine and orthopyroxene. Spinels are greenish brown and highly irregular in shape.

D-50 is a rare petrographic type among the Guatemalan peridotites (T. W. Donnelly, pers. comm., 1982). It is a pyroxenite, dominantly of orthopyroxene (0.5–6 mm), with lesser clinopyroxene (0.5–2 mm) and some interstitial olivine. The thin exsolution lamellae in the orthopyroxene are deformed, bent, and sheared off; lamellae in the clinopyroxene show evidence of the same deformation. There is minor green-brown spinel, rarely intergrown with orthopyroxene, and interstitial, anhedral olivines, which are extensively altered. The sample is veined and partially altered to serpentine and smectite.

MINERAL COMPOSITIONS

Mineral analyses were done on 26-mm-diameter polished sections with the CAMEBAX automated electron-probe microanalyzer at the Scripps Institution of Oceanography. Working conditions were 15 kV accelerating voltage and 15 nA sample current, with count times of 20 s. Spot size averaged 15 μm, but varied between 2 and 20 μm for some analyses.

Olivines in all samples have uniformly high concentrations of MgO and NiO, and low amounts of CaO (Table 4). The olivine in drilled samples cluster around $Fo_{90.8}$ and Fo_{92} (Fig. 2). The latter, very high number may reflect more extensive subsolidus reequilibration in 567A-29-2, 30–35 cm. Olivine compositions in the onshore samples, though very similar in Ni and Ca contents, are distinctly lower in Mg, ranging in composition from $Fo_{89.7}$ to $Fo_{90.5}$.

The pyroxenes in the drilled samples are also Mg-rich, plotting primarily in the diopside and enstatite fields (Fig. 2; Tables 5 and 6). The major variation in composition is in the Ca contents, as reflected in the spread of points parallel to the Wo–En join. The minerals in 567A-29-2, 30–35 cm, particularly the orthopyroxene, are slightly more Mg-rich than those in the other samples

Table 4. Selected analyses of olivine (oxides in wt.%, elements as atoms per 4 oxygens).

	567A-29-2, 30–35 cm		566C-6-1, 31–33 cm		CR 205		D-50		DL-90	
SiO_2	41.05	40.56	40.44	40.52	40.54	40.25	40.26	40.20	40.23	40.14
TiO_2	0.01	0.01	0.03	0.01	0.00	0.03	0.01	0.01	0.01	0.00
Al_2O_3	0.00	0.00	0.00	0.00	0.00	0.00	0.00	0.00	0.00	0.00
FeO	7.85	7.64	8.93	8.97	9.58	9.16	9.55	9.54	9.82	9.96
MnO	0.07	0.06	0.08	0.06	0.04	0.04	0.08	0.08	0.05	0.05
MgO	51.14	50.70	49.83	50.13	49.51	49.03	49.06	49.22	48.87	49.09
CaO	0.03	0.01	0.03	0.03	0.03	0.01	0.04	0.04	0.05	0.04
NiO	0.43	0.40	0.34	0.35	0.33	0.34	0.42	0.43	0.37	0.37
Cr_2O_3	0.02	0.00	0.02	0.03	0.03	0.03	0.00	0.00	0.01	0.01
Total	100.60	99.39	99.69	100.10	100.06	98.89	99.41	99.52	99.39	99.69
Si	0.993	0.992	0.991	0.990	0.993	0.996	0.993	0.991	0.993	0.989
Ti	0.000	0.000	0.000	0.000	0.000	0.000	0.000	0.000	0.000	0.000
Al	0.000	0.000	0.000	0.000	0.000	0.000	0.000	0.000	0.000	0.000
Fe^{+2}	0.159	0.156	0.182	0.183	0.196	0.189	0.197	0.196	0.202	0.205
Mn	0.001	0.001	0.002	0.001	0.000	0.000	0.001	0.001	0.000	0.001
Mg	1.844	1.849	1.821	1.825	1.808	1.808	1.805	1.808	1.799	1.804
Ca	0.000	0.000	0.000	0.000	0.000	0.000	0.000	0.001	0.001	0.001
Ni	0.008	0.007	0.007	0.006	0.006	0.006	0.008	0.008	0.007	0.007
Cr	0.000	0.000	0.000	0.000	0.000	0.000	0.000	0.000	0.000	0.000
FO	92.0	92.2	90.8	90.8	90.2	90.5	90.1	90.2	89.8	89.7

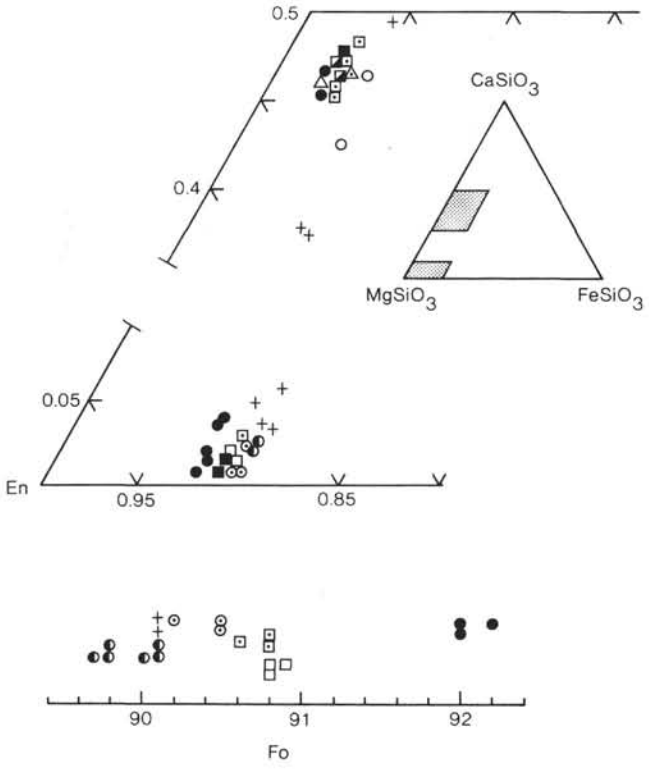

Figure 2. Olivine, orthopyroxene, and clinopyroxene compositions for onshore and drilled samples. Symbols as in Figure 3.

(Fig. 2). Orthopyroxenes have low TiO_2 contents (less than 0.04%), moderate Al_2O_3 (2.15–4.1%) and moderate Cr_2O_3 (0.57–1%) (Table 5). The clinopyroxenes likewise generally have Al_2O_3 in the range 1.8–2.9% and Cr_2O_3 of 0.5–1.0%, as well as low contents of Na_2O (Table 6). These mineral compositions are consistent with an interpretation of the serpentinite progenitor as a refractory mantle material. The pyroxene fragments were too small to evaluate effects of core–rim variation.

The pyroxenes in the onshore samples, though also Mg-rich, are distinct from the pyroxenes in the drilled samples in their consistently higher Fe contents (Fig. 2; Tables 5 and 6). In onshore sample D-50, the clinopyroxenes tend to be lower in Ca content and the orthopyroxenes significantly higher in Ca content than those in their drilled counterparts. Though their Cr contents are similar, the orthopyroxenes are consistently higher in Al_2O_3 content (4–6%). The clinopyroxenes have much higher abundances of Al_2O_3 (5.6–7.4%). Sample DL-90 also has clinopyroxenes with very high Al_2O_3 (7%), high TiO_2 (0.35–0.48%), and high Na_2O (0.8%) contents suggesting that these are much less refractory materials than those in the drilled samples. These compositions are distinct from most pyroxene analyses from alpine or oceanic-type peridotites, which have Na_2O contents in the range of 0.12–0.25% and Al_2O_3 contents of 1.5–5.5% (Sinton, 1979; Arai and Fujii, 1979; Clarke and Loubat, 1977). However, they are not as high in Na as jadeitic clinopyroxenes in eclogite xenoliths (Shee and Gurney, 1979), and are similar in some ways to pyroxene compositions from Cr-diopsied megacrysts in alkalic basalts (Jagoutz et al., 1979; Nixon and Boyd, 1979).

The spinels show the most distinct variations in chemical compositions of any of the relict minerals, as might be expected, since their complex chemistry makes them sensitive indicators of petrogenetic processes and conditions. The spinels in the drilled samples fall in the range of $Mg/Mg + Fe^{+2} = 0.55–0.67$ and $Cr/Cr + Al = 0.4–0.58$, again with the exception of 567A-29-2, 30–35 cm, in which the spinels have significantly lower Cr and Mg contents (Figs. 3 and 4; Table 7). All are low in Ti and Fe^{+3}, and there is a tendency to slightly higher Fe^{+3} with higher Cr contents (Fig. 4). Compositions within samples are uniform, and zoning is slight, tending to

Table 5. Selected analyses of orthopyroxene (oxides in wt.%, elements as atoms per 6 oxygens).

	566C-6-1, 31-33 cm		567A-29-2, 30-35 cm			570-42-1, 111-113 cm		CR 205		D 50		DL 90	
								Small	Core	Core	Rim	Core	Rim
SiO_2	55.42	55.44	54.06	54.80	54.83	55.02	54.92	54.13	52.87	53.38	53.49	53.21	53.38
TiO_2	0.03	0.02	0.02	0.04	0.04	0.03	0.04	0.10	0.11	0.05	0.04	0.11	0.17
Al_2O_3	2.15	2.22	4.10	3.75	3.98	2.40	1.86	4.68	5.66	4.63	4.75	5.50	5.26
FeO	6.01	5.87	5.09	4.94	5.10	5.77	5.81	6.32	5.96	5.88	6.51	6.19	6.23
MnO	0.08	0.07	0.12	0.06	0.05	0.09	0.05	0.06	0.08	0.10	0.08	0.08	0.09
MgO	34.12	33.85	33.56	33.50	34.42	34.39	34.52	33.48	32.19	31.29	31.74	31.76	31.94
CaO	1.15	1.58	0.77	1.97	0.40	0.56	0.63	0.29	1.19	3.10	1.66	1.35	1.34
Na_2O	—	—	0.02	—	—	—	—	—	—	—	—	—	—
K_2O	—	—	0.02	—	—	—	—	—	—	—	—	—	—
P_2O_5	—	—	0.00	—	—	—	—	—	—	—	—	—	—
NiO	0.06	0.14	0.15	0.11	0.12	0.06	0.12	0.13	0.09	0.09	0.09	0.13	0.07
Cr_2O_3	0.57	0.62	1.05	1.00	0.90	0.59	0.43	0.49	0.66	1.01	0.99	0.69	0.58
Total	99.59	99.81	98.97	100.15	99.85	98.90	98.38	99.68	98.81	99.53	99.35	94.01	99.07
Si	1.926	1.924	1.886	1.892	1.891	1.920	1.929	1.878	1.854	1.870	1.873	1.863	1.868
Ti	0.001	0.001	0.001	0.000	0.001	0.001	0.001	0.003	0.003	0.001	0.001	0.003	0.004
Al IV	0.073	0.075	0.114	0.107	0.108	0.079	0.070	0.121	0.145	0.129	0.126	0.136	0.131
Al VI	0.013	0.014	0.054	0.044	0.053	0.019	0.005	0.069	0.088	0.061	0.069	0.090	0.085
Fe^{+2}	0.174	0.170	0.148	0.142	0.147	0.168	0.171	0.183	0.174	0.172	0.190	0.181	0.182
Mn	0.002	0.002	0.004	0.001	0.001	0.003	0.001	0.002	0.002	0.003	0.002	0.002	0.003
Mg	1.768	1.751	1.745	1.723	1.769	1.789	1.807	1.731	1.682	1.634	1.657	1.658	1.667
Ca	0.043	0.059	0.028	0.072	0.015	0.020	0.023	0.011	0.044	0.115	0.062	0.050	0.049
Na	—	—	0.002	—	—	—	—	—	—	—	—	—	—
K	—	—	0.001	—	—	—	—	—	—	—	—	—	—
P	—	—	0.000	—	—	—	—	—	—	—	—	—	—
Ni	0.002	0.004	0.004	0.002	0.003	0.002	0.003	0.004	0.002	0.002	0.003	0.004	0.002
Cr	0.016	0.017	0.028	0.026	0.024	0.016	0.012	0.013	0.018	0.028	0.027	0.019	0.016
Wo	2.1	2.9	1.5	3.7	0.7	1.0	1.1	0.005	2.3	5.9	3.2	2.6	2.5
En	89.0	88.4	90.8	88.9	91.6	90.4	90.3	89.9	88.5	85.0	86.7	87.7	87.8
Fs	8.7	8.5	7.7	7.3	7.6	8.4	8.5	9.5	9.1	8.9	9.9	9.5	9.5

Note: Small denotes analyses of grains on same order of size as spot (generally less than 30 μm); core and rim denote, respectively, analyses of the center and edge of larger grains; notation in subsequent tables is the same. — indicates not determined.

Table 6. Selected analyses of clinopyroxene (oxides in wt.%, elements as atoms per 6 oxygens).

	566-9-1, 9-11 cm		566C-6-1, 31-33 cm		570-42-1, 111-113 cm		D 50		DL 90	
							Rim	Core	Core	Rim
SiO_2	53.19	52.30	52.72	52.71	52.78	52.48	51.41	51.60	51.61	50.27
TiO_2	0.12	0.09	0.03	0.07	0.05	0.04	0.13	0.10	0.35	0.48
Al_2O_3	1.83	2.02	2.55	2.91	2.51	1.91	5.73	5.62	7.08	7.41
FeO	1.69	2.19	2.21	2.19	1.95	2.00	3.64	3.79	3.11	2.89
MnO	0.10	0.07	0.04	0.09	0.11	0.09	0.10	0.12	0.15	0.15
MgO	18.10	18.24	17.70	17.80	17.76	17.88	20.11	19.84	17.06	15.62
CaO	22.99	23.98	23.28	23.08	23.39	23.09	18.84	18.27	19.22	20.77
Na_2O	0.14	—	0.04	0.02	0.03	0.04	0.04	0.08	0.88	0.83
K_2O	0.00	—	0.02	0.01	0.00	0.02	0.01	0.02	0.00	0.01
P_2O_5	0.00	—	0.03	0.00	0.01	0.02	0.03	0.01	0.00	0.00
NiO	0.07	0.09	0.08	0.04	0.07	0.09	0.15	0.08	0.07	0.03
Cr_2O_3	0.89	0.08	0.84	1.14	0.90	0.55	1.24	1.27	1.09	1.08
Total	99.11	99.85	99.54	100.05	99.55	98.21	101.42	100.80	100.62	99.54
Si	1.944	1.911	1.924	1.914	1.925	1.938	1.835	1.849	1.852	1.832
Ti	0.003	0.002	0.001	0.002	0.001	0.001	0.002	0.002	0.008	0.013
Al IV	0.056	0.087	0.075	0.085	0.074	0.061	0.164	0.150	0.147	0.167
Al VI	0.023	0.000	0.034	0.038	0.033	0.021	0.076	0.087	0.151	0.151
Fe^{+2}	0.052	0.067	0.067	0.066	0.059	0.061	0.108	0.113	0.093	0.087
Mn	0.003	0.002	0.001	0.003	0.003	0.003	0.002	0.003	0.004	0.005
Mg	0.986	0.992	0.962	0.963	0.965	0.984	1.070	1.060	0.912	0.849
Ca	0.900	0.938	0.910	0.898	0.914	0.914	0.720	0.701	0.739	0.811
Na	0.010	—	0.003	0.001	0.002	0.003	0.002	0.005	0.061	0.058
K	0.000	—	0.001	0.000	0.000	0.001	0.000	0.000	0.000	0.000
P	0.000	—	0.001	0.000	0.000	0.001	0.000	0.000	0.000	0.000
Ni	0.002	0.003	0.002	0.001	0.002	0.003	0.003	0.001	0.001	0.001
Cr	0.025	0.025	0.024	0.033	0.026	0.016	0.034	0.035	0.030	0.031
Wo	46.4	46.9	46.9	46.6	47.1	46.6	37.9	37.4	42.3	46.4
En	50.9	49.6	49.6	49.9	49.7	50.2	56.3	56.5	52.2	48.5
Fs	2.7	3.3	3.4	3.4	3.0	3.1	5.6	6.0	5.3	4.9

Note: See note to Table 5.

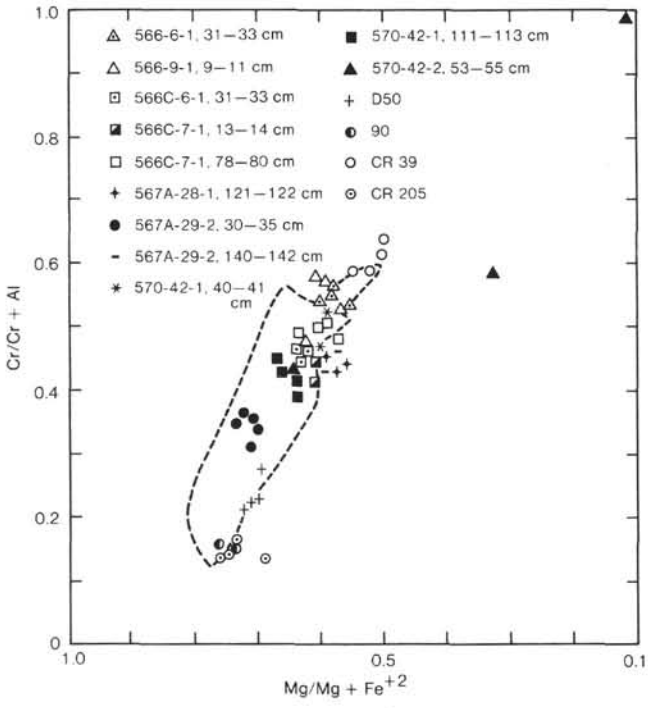

Figure 3. Cr/Cr + Al vs. Mg/Mg + Fe^{+2} for relict spinels in onshore and drilled samples. Dotted field is that of spinels from abyssal peridotites, after Dick and Bullen (in press).

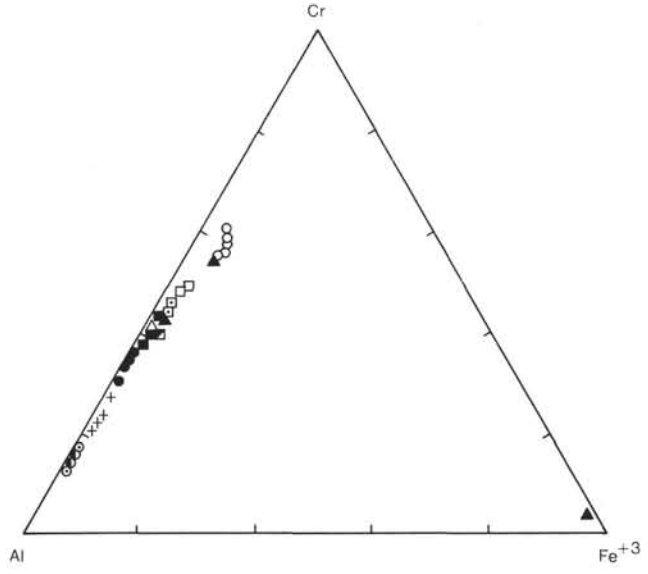

Figure 4. Trivalent constituents of spinels from onshore and drilled samples. Symbols as in Figure 3; for clarity, only selected analyses are plotted.

rims less Cr-rich than cores. In some cases alteration of the spinels has produced black rims of magnetite and compositions intermediate between the Cr-spinel, ferrichromite, and magnetite (Fig. 4).

The three least-serpentinized onshore samples have Al-rich spinels, as suggested by their greenish black color in thin section. Those of D-50 are closest to 567A-29-2, 30–35 cm in composition; these have low Ti contents as well. The spinels in CR 39 are the most Cr-rich of any sampled; they occur, however, in a totally serpentinized and slightly deformed breccia, and it is not clear that these are indeed primary compositions. Alteration of spinels will tend to drive them to higher Cr and Fe contents, generally like the ferrichromite compositions in 570-42-2, 53–55 cm (Fig. 4). The extensive serpentinization and deformation in this sample make its interpretation as a primary composition suspect.

Although diverse in composition, most of the spinels analyzed have Cr/Cr + Al ratios less than 0.60. The compositions of spinels in the Leg 84 serpentinites, though not definitely of oceanic character, fall within the range of compositions found for spinels in abyssal peridotites (Aumento and Loubat, 1971; Sigurdsson, 1977; Arai and Fujii, 1979; Dick and Bullen, in press). The onshore samples, though distinct from the drilled samples, fall in the range of abyssal peridotite compositions as well. The peridotites at Santa Elena are associated with basalts that have been interpreted as ocean-ridge tholeiites (Weyl, 1969; Pichler and Weyl, 1975), and with gabbros which have common cumulate olivine and poikilitic orthopyroxene (Galli-Olivier, 1979; Azéma and Tournon, 1982), both common characteristics of ocean-ridge gabbros (Hodges and Papike, 1976; Tiezzi and Scott, 1980).

Geothermometry using the analyzed mineral compositions indicates that there has been subsolidus reequilibration in these samples. The olivine–spinel geothermometer calibration of Roeder et al. (1979) gives temperatures of 730–850°C for the drilled samples and 820–990°C for the onshore samples. Despite the differences in mineral composition between Sample 567A-29-2, 30–35 cm and the other drilled samples, calculated temperatures for all are similar, suggesting that the differences reflect initially distinct compositions rather than differing degrees of reequilibration. Mori's (1977) calibration of the two-pyroxene geothermometer indicates temperatures of 1110–1170°C for the drilled samples, much closer to those expected for mantle materials, but still indicative of some reequilibration. The onshore samples yield temperatures of 1220–1440°C; like the olivine–spinel calculations, these temperatures are higher than those calculated for the drilled samples.

DISCUSSION

The petrography of the serpentinites drilled on Leg 84 indicates that they were clinopyroxene-bearing harzburgites before serpentinization. Their mineral chemistry is refractory: high-Mg olivines (Fo_{91-92}) and orthopyroxene (En_{89-91}); low-Ti and -Fe^{+3} spinels and low-Al and -Na pyroxenes. Such compositions are considered characteristic of rocks interpreted to be upper-mantle materials residual from an episode of partial melting (Menzies, 1977; England and Davies, 1973; Loney et al., 1971). Sample 567A-29-2, 30–35 cm is distinct from the remainder of the samples in its more magnesian olivines and orthopyroxene and more aluminous spinels. Beyond suggesting a mantle affinity for these materials, it is difficult to be more specific about their origin. Their mineral compositions, particularly those of the spinels, are similar to those reported for peridotites from the ocean

Table 7. Selected analyses of spinels (oxides in wt.%, elements as atoms per 32 oxygens).

	566-9-1, 9-11 cm			567A-28-1, 121-122 cm		567A-29-2, 30-35 cm		566C-6-1, 31-33 cm			570-42-1, 111-113 cm			570-42-2, 53-55 cm			CR 39		CR 205		D 50		DL 90	
	Core	Rim	Small	Core	Rim	Small	Core	Core	Rim	Core	Core	Rim	Small	Core	Core	Core	Core	Rim	Core	Core	Core	Core	Core	Core
SiO_2	0.00	0.00	0.01	0.00	0.00	0.00	0.01	0.00	0.00	0.00	0.00	0.00	0.00	0.00	0.00	0.00	0.17	0.00	0.00	0.00	0.00	0.00	0.00	0.03
TiO_2	0.11	0.16	0.15	0.12	0.04	0.05	0.08	0.06	0.09	0.06	0.05	0.08	0.08	0.08	0.02	0.05	0.13	0.14	0.05	0.06	0.09	0.03	0.09	0.08
Al_2O_3	23.12	23.46	25.75	31.16	32.12	40.18	39.27	32.25	30.48	30.66	31.91	33.68	34.36	30.19	0.00	32.60	19.61	19.62	54.11	56.09	43.89	50.12	54.29	53.46
Fe_2O_3	2.92	2.74	3.08	1.39	1.56	0.50	0.78	1.85	2.28	2.23	1.93	1.03	1.67	2.06	67.72	1.31	4.31	4.88	0.61	0.70	1.10	0.76	0.83	1.38
FeO	16.21	16.80	17.17	17.67	17.33	12.87	12.58	15.39	15.13	15.08	13.71	14.34	15.02	15.21	31.56	14.87	19.10	19.07	12.08	11.57	13.24	12.38	11.84	11.01
MnO	0.20	0.15	0.23	0.14	0.13	0.20	0.18	0.21	0.17	0.18	0.13	0.14	0.17	0.12	0.03	0.17	0.16	0.20	0.08	0.07	0.13	0.08	0.10	0.07
MgO	12.87	12.76	12.64	12.65	12.97	16.81	17.05	14.48	14.47	14.53	15.45	15.22	14.87	14.55	0.09	14.74	10.65	10.40	18.89	19.34	16.82	17.96	18.86	18.94
CaO	0.01	0.02	0.04	0.01	0.03	0.02	0.03	0.02	0.01	0.02	0.03	0.01	0.01	0.02	0.03	0.06	0.03	0.00	0.00	0.00	0.01	0.08	0.01	0.02
NiO	0.08	0.04	0.08	0.08	0.10	0.06	0.07	0.15	0.12	0.19	0.09	0.09	0.10	0.07	0.13	0.13	0.07	0.10	0.26	0.27	0.18	0.36	0.31	0.31
Cr_2O_3	45.74	45.21	42.63	37.15	36.67	30.63	31.88	37.88	39.17	39.46	38.20	36.82	35.44	40.33	2.99	37.80	46.45	45.75	15.96	13.52	25.24	19.44	14.34	14.20
Total	101.27	101.85	101.69	100.48	100.96	101.33	101.91	102.29	101.93	102.39	101.50	101.41	101.72	102.61	102.57	101.74	100.66	100.16	102.04	101.61	100.71	101.21	100.95	99.52
Si	0.000	0.000	0.005	0.000	0.000	0.000	0.000	0.000	0.000	0.000	0.000	0.000	0.000	0.000	0.000	0.000	0.044	0.000	0.000	0.000	0.000	0.000	0.000	0.005
Ti	0.021	0.027	0.027	0.022	0.005	0.010	0.010	0.010	0.016	0.010	0.005	0.010	0.010	0.016	0.005	0.010	0.027	0.027	0.016	0.010	0.106	0.006	0.016	0.011
Al VI	6.627	6.819	7.282	8.737	8.899	10.515	10.258	8.758	8.360	8.366	8.680	9.115	9.273	8.236	0.000	8.859	5.814	5.853	13.259	13.661	11.390	12.591	13.464	13.364
Fe^{+3}	0.535	0.498	0.557	0.248	0.275	0.084	0.130	0.320	0.398	0.388	0.335	0.178	0.287	0.359	15.277	0.227	0.815	0.930	0.096	0.109	0.182	0.122	0.130	0.221
Fe^{+2}	3.296	3.392	3.435	3.503	3.404	2.391	2.329	2.964	2.942	2.921	2.647	2.751	2.875	2.944	7.915	2.867	4.018	4.040	2.102	1.998	2.437	2.204	2.069	1.954
Mn	0.043	0.032	0.043	0.027	0.027	0.038	0.032	0.043	0.032	0.037	0.021	0.027	0.032	0.021	0.005	0.032	0.033	0.044	0.010	0.010	0.022	0.016	0.016	0.011
Mg	4.665	4.591	4.526	4.474	4.546	5.565	5.632	4.970	5.019	5.013	5.314	5.209	5.075	5.023	0.042	5.066	3.992	3.926	5.854	5.957	5.518	5.706	5.881	5.988
Ca	0.000	0.005	0.010	0.000	0.005	0.005	0.005	0.005	0.000	0.005	0.005	0.005	0.005	0.005	0.010	0.016	0.005	0.000	0.000	0.000	0.005	0.016	0.000	0.005
Ni	0.016	0.005	0.016	0.016	0.022	0.010	0.010	0.027	0.021	0.032	0.016	0.016	0.021	0.016	0.031	0.027	0.016	0.016	0.043	0.043	0.033	0.060	0.049	0.056
Cr	8.793	8.628	8.094	6.969	6.813	5.378	5.589	6.899	7.208	7.223	6.972	6.683	6.417	7.382	0.711	6.892	9.236	9.159	2.622	2.206	4.393	3.274	2.371	2.379
Cr/Cr + Al	0.570	0.558	0.526	0.443	0.433	0.338	0.352	0.440	0.463	0.463	0.445	0.423	0.408	0.472	1.000	0.437	0.613	0.610	0.165	0.139	0.278	0.206	0.149	0.151

Note: See note to Table 5.

basins. There is no evidence (i.e., high-Cr spinels or a dominantly clinopyroxene-free harzburgite assemblage) that might indicate a very refractory, or island-arc type association (Dick and Bullen, in press).

With the exception of CR 39, the onshore set of samples from Guatemala and Costa Rica are a distinctly different assemblage from drilled samples. They are also akin to materials of upper-mantle origin, but have more aluminous spinels, more Fe-rich olivines and pyroxenes, and more sodic and aluminous clinopyroxenes than the Leg 84 samples. Though CR 205 and DL-90 are cpx-bearing harzburgites, and are texturally similar to the Leg 84 samples, they are chemically less depleted rocks. D-50 has an apparently cumulate texture with large orthopyroxene and interstitial olivine, but has very magnesian mineral compositions and low-Ti, low-Fe^{+3} spinels which may indicate a mantle origin. This sample could be a fragment of a pyroxenite dike or pod of upper-mantle origin. The Al and Na contents of the clinopyroxenes in all the onshore samples are higher than is characteristic of pyroxenes described from oceanic fracture zones or ophiolites thought to be fragments of ocean crust (Arai and Fujii, 1979; Pallister and Hopson, 1981; Aumento and Loubat, 1971; Dick and Bullen, in press). The sample is not large, however, and the onshore samples are similar enough in composition to the oceanic samples that they might be less-depleted oceanic mantle materials.

Although it is clear that the Leg 84 samples are distinct from the onshore samples, nothing in the data prohibits a general relationship between the two. Both onshore suites could be materials derived from the oceanic mantle. Peridotite sections in ophiolites can vary greatly on both large and small scales (Boudier and Coleman, 1981; Evans, 1983). The Leg 84 sample set is fairly uniform over the area sampled; the onshore samples are limited in number, come from a substantial distance from the drill sites, and may be biased toward more atypical varieties because they were generally the least serpentinized samples available. What is intriguing is that the sample from Costa Rica (CR 205) and the samples from Guatemala (DL-90 and D-50) have quite similar mineral compositions, suggesting that both were formed from similar sources and by similar processes, and that those chemical compositions may be neither unusual nor unrepresentative. The compositional differences between the two samples sets (onshore and offshore) may represent two distinct and possibly unrelated types of mantle material.

If the drilled samples are indeed mantle materials and of ocean-crustal origin, they must have come from depths of 9–12 km, judging by the occurrence of similar harzburgitic rocks in ophiolites and the depth to the Moho in seismic sections of ocean crust (Clague and Straley, 1977). This raises the question of why these serpentinized peridotites are now exposed at relatively shallow depths throughout the trench slope. There are at least two likely ways such exposures might occur: (1) imbricate faulting of slices of ocean crust, or (2) diapirism of serpentinized ultramafics along zones of weakness in the trench slope.

Seismic profiles of the forearc have been interpreted as showing two or more large imbricate slices of ocean crust in the forearc (Ladd et al., 1978). Such imbricate stacking might well expose some upper mantle materials at shallow depths. There are, however, some aspects of the drilled assemblages which contradict a model based only on imbricate stacking. As pictured by Ladd et al. (1978) or Azéma and Tournon (1982, p. 740), the most common materials sampled ought to be basalts, diabases, and gabbros, with lesser amounts of peridotitic rocks. In contrast, coring recovered serpentinite as the sole basement rock at Holes 566, 566A, 566C, and 570; serpentinite in blocks and between units of basalt and gabbro in Hole 567A; and gabbro and basalt alone in Hole 569A (site chapters, this volume). Furthermore, the common association reported in dredge and piston core samples is serpentinite, basalt, and chert (Ibrahim et al., 1979); gabbro is notably lacking from these sets of samples. The coarser-grained samples from Leg 84 are predominantly altered, massive gabbro or diabase, rather than cumulate-textured gabbros. The existing sample set seems strongly biased toward serpentinite, with lesser amounts of basalt and diabase, and minor volumes of gabbro. This bimodal distribution would be surprising in a simple set of stacked crustal sheets.

The other fact that should be noted is that the "serpentinized peridotites" are really serpentinites—greater than 90% serpentine and secondary minerals. Serpentine is a relatively mobile material; it is found at very shallow depths in fracture zones (e.g., Bonatti, 1976), where its emplacement is usually inferred to be diapiric; it also occurs as diapiric bodies in many deformed terranes (e.g., the Franciscan Formation of California; Oakeshott, 1968). In northern Central America there are bodies of serpentinite along many of the high- and low-angle faults in the region (King, 1968; Anderson et al., 1973; Weyl, 1980). Two requirements for such diapiric emplacement of serpentine may include (1) a source of water to circulate into mantle to alter the peridotite, and (2) a zone of weakness in the crust, such as a fault, along which the serpentine can be emplaced, driven presumably by its low density and aided by its relative mobility. The forearc along the Leg 67 and Leg 84 transects would appear to satisfy both conditions. There should be faults developed as a result of the presumed initial imbrication of crustal materials in the forearc. There is also a complex network of high-angle faults throughout northern Central America, which probably extends into the forearc. If this is the case, these faults provide both zones of weakness in the crust and pathways along which water can circulate into the lower crust and mantle to produce the serpentinites. Dehydration of sediments and altered igneous rocks as they are subducted beneath the forearc may also contribute water to the system.

Serpentine diapirism in the forearc may explain the distribution of basement rocks at the drill sites. Where diapirs pierce the upper crustal layers, the basement would consist solely of serpentine; where they had simply pushed into and fractured the upper crust, a complex mixture of basalts, diabases, and serpentine might be found. Such diapirism could explain the bimodal distribution of rock

samples in the trench slope. There is some morphologic and seismic evidence to support the suggestion that serpentine diapirism is, or was, important in the forearc. Seely (1979) noted shallow magnetic bodies and cross-cutting structures in seismic reflection lines across the Guatemalan margin, which he interpreted as serpentine diapirs of shallow slices of ocean crust. An indication that sediments were dragged upward at the edges of the structures favored the former (Seely, 1979). There is a great deal of relief in the basement topography (site chapters), some of which could be due to diapirism. Serpentine diapirs are commonly "elliptical and slightly elongate in plan" (Oakeshott, 1968), and there are a number of conical or slightly elongate, elliptical features on the trench slope. The Seabeam map of Aubouin et al. (1982, p. 736) shows several conical and elliptical bathymetric highs in the forearc which are often elongate subparallel to the trench axis (for example, near 12°43′N, 90°47′W and 12°50′N, 90°54′W). Near Site 570 there is a conical high closely corresponding to a magnetic high (Volpe, this volume). This feature may well be a diapiric structure cored by serpentine. The magnetic characteristics of serpentine are highly variable, and are probably not reliable in mapping such bodies—the highly variable development of secondary oxides in the samples described here is probably the primary cause of such variation. The fact that serpentine was recovered at such a high proportion of sites may in part reflect a tendency to drill basement highs where the sediment cover is thinner; Site 570, for example, clearly sits atop such a basement high (site chapter, this volume). Diapiric structures would be expected to be areas of positive relief in the basement.

Diapirism of serpentinites in other trench slope and forearc regions has been described. The inner slope of the Mariana Trench between 16° and 18°N is characterized by very large amounts of serpentinite and serpentinized peridotites (Bloomer and Hawkins, 1983). There are elongate bathymetric highs along the trench-slope break, sometimes referred to as forearc seamounts (Hussong and Fryer, 1982). Dredge hauls along these yielded primarily serpentine and volcaniclastic siltstones. These have been interpreted as diapirs piercing the volcanic basement surrounding them (Bloomer, 1983). The geologic setting in the Marianas forearc is certainly different from that off Guatemala, in that the forearc basement in the Marianas is clearly of island-arc origin. Regardless of the difference in setting, if there is extensive, deep faulting in the forearc and ultramafic rocks at depth, serpentine diapirism is likely to become an important process.

The suggestion of diapirism of serpentine in the forearc along the Leg 84 transect does not negate the possibility of imbricate faulting. Such diapirism might have accompanied the disruption and faulting of the crustal materials, or could have occurred after that faulting.

CONCLUSIONS

1. The serpentinites sampled on Leg 84 are derived from clinopyroxene-bearing harzburgites with mineral compositions characteristic of upper-mantle rocks depleted to some extent by an epsiode of partial melting (olivine, $Fo_{90.6-92}$; orthopyroxene En_{89-91}; clinopyroxene $Wo_{47}En_{50}Fs_3$; spinel, Cr/Cr + Al = 0.3–0.6). The samples from all sites are relatively homogeneous, except for 567A-29-2, 30–35 cm, which has more magnesian olivines and orthopyroxenes and more aluminous spinels than the other drilled samples.

2. The least-serpentinized samples from ultramafic exposures in Costa Rica and Guatemala, two of which were clinopyroxene-bearing harzburgites, have mineral chemistries distinct from those of the drilled samples. Their more iron-rich olivines and pyroxenes, aluminous spinels, and sodic and aluminous clinopyroxenes indicate that these are less-depleted materials than the Leg 84 samples. CR 39, a serpentinite, has spinel compositions more Cr-rich than those of the Leg 84 samples, but it is not clear that these represent unaltered relict compositions.

3. Both the onshore and the offshore sets of samples could be derived from oceanic-type mantle—that beneath an ocean-crustal section formed at a spreading ridge. It is unclear, however, whether the offshore and onshore ultramafics are parts of a related terrane.

4. Diapirism of serpentine may have been an important process in the development of the forearc. This might account for the abundance of serpentine in the recovered materials, the bimodal distribution of rock types in dredged and drilled samples (serpentine and basalt), and some of the morphologic characteristics of the trench slope and forearc.

ACKNOWLEDGMENTS

M. Baltuck assisted greatly in obtaining the Leg 84 samples, and T. W. Donnelly and N. Lundburg kindly provided samples from Guatemala and Costa Rica, respectively. A. Volpe and M. Baltuck provided several helpful discussions. R. Fujita assisted with the microprobe analyses. Reviews by T. W. Donnelly and C. Evans greatly improved the manuscript. This work was supported by a grant from the Scripps Industrial Associates.

REFERENCES

Anderson, T. H., Burkart, B., Clemons, R. E., Bohnenger, O. H., and Blount, D. N., 1973. Geology of the western Altos Cuchumatanes, northwestern Guatemala. *Geol. Soc. Am. Bull.*, 84:805–826.

Arai, S., and Fujii, T., 1979. Petrology of ultrabasic rocks from Site 395. *In* Melson, W. G., Rabinowitz, P. D., et al., *Init. Repts. DSDP*, 45: Washington (U.S. Govt. Printing Office), 587–594.

Aubouin, J., Stephan, J., Renard, V., Roump, J. and Lonsdale, P., 1982. A Seabeam survey of the Leg 67 area (Middle America Trench off Guatemala). *In* Aubouin, J., von Huene, R., et al., *Init. Repts. DSDP*, 67: Washington (U.S. Govt. Printing Office), 733–745.

Aumento, F., and Loubat, H., 1971. The Mid-Atlantic Ridge near 45°N XVI. Serpentinized ultramafic intrusions. *Can. J. Earth. Sci.*, 8:631–663.

Azéma, J., and Tournon, J., 1982. The Guatemala margin, the Nicoya Complex, and the origin of the Caribbean Plate. *In* Aubouin, J., von Huene, R., et al., *Init. Repts. DSDP*, 67: Washington (U.S. Govt. Printing Office), 739–745.

Bloomer, S. H., 1983. Distribution and origin of igneous rocks from the landward slopes of the Mariana Trench: implications for its structure and evolution. *J. Geophys. Res.*, 88:7411–7428.

Bloomer, S. H., and Hawkins, J. W., 1983. Gabbroic and ultramafic rocks from the Mariana Trench: an island arc ophiolite. *In* Hayes, D. E. (Ed.), *The Tectonic and Geologic Evolution of Southeast Asian Seas and Islands*, II. Am. Geophys. Union (Washington), Geophys. Mono., 27:294–317.

Bonatti, E., 1976. Serpentinite protrusions in the oceanic crust. *Earth Planet. Sci. Lett.*, 32:107–113.

Boudier, F., and Coleman, R. G., 1981. Cross-section through the peridotite in the Semail ophilite, southeastern Oman mountains. *J. Geophys. Res.*, 86:2573–2592.

Clague, D., and Straley, P., 1977. Petrologic nature of the oceanic Moho. *Geology*, 5:133–136.

Clarke, D. B., and Loubat, H., 1977. Mineral analyses from the peridotite–basalt–gabbro complex at Site 334, DSDP Leg 37. *In* Aumento, F., Melson, W. G., et al., *Init. Repts. DSDP*, 37: Washington (U.S. Govt. Printing Office), 847–857.

Couch, R., 1976. Estructuras del margén continental de Centro America y el desarollo de una hipótesis. *In* Perez-Rodrequez, R., and Suarez-Zozaya, M. R. (Eds.), *First Reunion Latino-Americano sobre Ciencia Tecnologia de los Oceanos*: Mexico (Secretaria de Marina Mexicana), pp. 120–139.

Couch, R., and Woodcock, S., 1981. Gravity and structure of the continental margins of southwestern Mexico and northwestern Guatemala. *J. Geophys. Res.*, 86:1829–1840.

Coulbourn, W. T., Hesse, R., Azema, J., and Shiki, T., 1982. A summary of the sedimentology of Deep Sea Drilling Project Leg 67 sites: the Middle America Trench and slope off Guatemala—an active margin transect. *In* Aubouin, J., von Huene, R., et al., *Init. Repts. DSDP*, 67: Washington (U.S. Govt. Printing Office), 759–774.

Dick, H. J. B., and Bullen, T., in press. Chromium spinel as a petrogenetic indicator in oceanic environments. *Contrib. Mineral. Petrol.*

England, R. L., and Davies, H. L., 1973. Mineralogy of ultramafic cumulates and tectonites from eastern Papua. *Earth Planet. Sci. Lett.*, 17:416–425.

Evans, C. A., 1983. Petrology and geochemistry of the transition from mantle to crust beneath an island arc–backarc pair: implications from the Zambales Range ophiolite, Luzon, Philippines [unpubl. Ph.D. dissertation]. Univ. Calif., San Diego.

Galli-Olivier, C., 1979. Ophiolite and island-arc volcanism in Costa Rica. *Geol. Soc. Am. Bull.*, 90:444–452.

Hodges, F. N., Papike, J. J., 1976. DSDP Site 334: magmatic cumulates from oceanic Layer 3. *J. Geophys. Res.*, 81:4135–4151.

Hussong, D. M., and Fryer, P., 1982. Structure and tectonics of the Mariana arc and forearc. Drillsite selection surveys. *In* Hussong, D. M., Uyeda, S., et al., *Init. Repts. DSDP*, 60: Washington (U.S. Govt. Printing Office), 33–44.

Ibrahim, A. K., Latham, G. V., and Ladd, J., 1979. Seismic refraction and reflection measurements in the Middle America Trench offshore Guatemala. *J. Geophys. Res.*, 84:5643–5649.

Jagoutz, E., Lorenz, V., and Wanke, H., 1979. Major-trace elements of Al-augites and Cr-diopsides from ultramafic nodules in European alkali basalts. *In* Boyd, F. R., and Meyer, H. O. A. (Eds.), *The mantle Sample: Inclusions in Kimberlites and Other Volcanics. Proc. Second Int. Kimberlite Conf.* (Vol. 2): Washington, (Am. Geophys. Union), 382–390.

King, P. B., 1968 (compiler). Tectonic map of North America, U.S. Geol. Survey Map.

Kuijpers, E., 1980. The geological history of the Nicoya ophiolite complex, Costa Rica, and its geotectonic significance. *Tectonophysics*, 68:233–255.

Ladd, J. W., Ibrahim, A. K., McMillen, K. J., Latham, G. V., von Huene, R. E., Watkins, J. E., Moore, J. C., and Worzel, J. L., 1978. Tectonics of the Middle America Trench offshore Guatemala. *Int. Symp. Guatemala 4 February Earthquake and Reconstruction Process* (Guatemala City, May 1978), Vol. 1.

Lawrence, D. P., 1975. Petrology and structural geology of the Sanarte–El Progreso area, Guatemala [unpubl. Ph.D. dissertation]. SUNY, Binghamton.

Loney, R. A., Himmelburg, G. R., and Coleman, R. G., 1971. Structure and petrology of the alpine-type peridotite at Burro Mountain, California, U.S.A. *J. Petrol.*, 12:245–309.

Maury, R. C., Bougault, H., Joron, J. L., Girard, D., Treuil, M., Azéma, J., and Aubouin, J., 1982. Volcanic rocks from the Leg 67 sites: mineralogy and geochemistry. *In* Aubouin, J., von Huene, R., et al., *Init. Repts. DSDP*, 67: Washington (U.S. Govt. Printing Office), 557–576.

Menzies, M., 1977. Residual alpine lherzolites and harzburgites—geochemical and isotopic constraints on their origin. *In* Dick, H. J. B. (Ed.), *Chapman Conference on Partial Melting in the Earth's Upper Mantle*. Oregon Dept. Geol. Min. Indus. Bull., 96:129–147.

Mori, T., 1977. Geothermometry of spinel lherzolites. *Contrib. Mineral. Petrol.*, 59:261–279.

Nixon, P. H., and Boyd, F. R., 1979. Garnet bearing lherzolites and discrete nodule suites from the Malaita alnoite, Solomon Islands, southwest Pacific and their bearing on oceanic mantle composition and geotherm. *In* Boyd, F. R., and Meyer, H. O. A. (Eds.), *The Mantle Sample: Inclusions in Kimberlites and Other Volcanics. Proc. Second Int. Kimberlite Conf.* (Vol. 2): Washington (Am. Geophys. Union), 400–423.

Oakeshott, G. B., 1968. Diapiric structures in the Diablo Range, California. *In* Braunstein, J., and O'Brien, G. D. (Eds.), *Diapirs and Diapirism*. Mem. Am. Assoc. Pet. Geol., 8:228–243.

Pallister, J., and Hopson, C. A., 1981. Samail ophiolite plutonic suite: field relations, phase variations, cryptic variation and layering, and a model of a spreading ridge magma chamber. *J. Geophys. Res.*, 86: 2593–2644.

Pichler, H., and Weyl, R., 1975. Magmatism and crustal evolution in Costa Rica. *Geol. Rundschau*, 64:457–475.

Roeder, P., Campbell, I., and Jamieson, H., 1979. A re-evaluation of the olivine-spinel geothermometer. *Contrib. Mineral. Petrol.*, 68: 325–334.

Rosenfeld, J. H., 1981. Geology of the western Sierra de Santa Cruz, Guatemala, Central America: an ophiolite sequence [unpubl. Ph.D. dissertation]. SUNY, Binghamton.

Seely, D. R., 1979. Geophysical investigations of continental slopes and rises. *In* Watkins, J. S., and Montadert, L. (Eds.), *Geological and Geophysical Investigations of Continental Margins*. Mem. Am. Assoc. Pet. Geol., 29:245–260.

Seely, D. R., Vail, P. R., and Walton, G. C., 1974. Trench slope model. *In* Burk, C. A., and Drake, C. L. (Eds.), *The Geology of Continental Margins*: New York (Springer-Varlag), pp. 249–260.

Shee, S. R., and Gurney, J. J., 1979. The mineralogy of xenoliths from Orapa, Botswana, *In* Boyd, F. R., and Meyer, H. O. A. (Eds.), *The Mantle Sample: Inclusions in Kimberlites and Other Volcanics*. Proc. Second Int. Kimberlite Conf., (Vol. 2): Washington, (Am. Geophy. Union), 37–49.

Sigurdsson, H., 1977. Spinels in Leg 37 basalts and peridotites: phase chemistry and zoning. *In* Aumento, F., Melson, W. G., et al., *Init. Repts. DSDP*, 37: Washington (U.S. Govt. Printing Office), 883–892.

Sinton, J. M., 1979. Petrology of (alpine-type) peridotites from Site 395, DSDP Leg 45. *In* Melson, W. G., Rabinowitz, P. D., et al., *Init. Repts. DSDP*, 45: Washington (U.S. Govt. Printing Office), 595–602.

Tiezzi, L. J., and Scott, R. B., 1980. Crystal fractionation in cumulate gabbro, Mid-Atlantic Ridge, 26°N. *J. Geophys. Res.*, 85:5438–5454.

von Huene, R., Aubouin, J., Azéma, J., Blackinton, G., Carter, J. H., et al., 1980. DSDP Mid-America Trench transect off Guatemala. *Geol. Soc. Am. Bull.*, 91, Pt. 1:421–432.

Weyl, R., 1969. Magmatische forderphasen und gesteinchemismus in Costa Rica. *Neues. Jahrb. Geol. Palaeontol. Monatsh.*, 7:423–446.

_____, 1980. *Geology of Central America*: Berlin (Gebruder Borntraeger).

Woodcock, S. F., 1975. Crustal structure of the Tehuantepec Ridge and adjacent continental margin of southwestern Mexico and western Guatemala [unpubl. Master's thesis]. Oregon State University.